

PCCP

Accepted Manuscript



This is an *Accepted Manuscript*, which has been through the Royal Society of Chemistry peer review process and has been accepted for publication.

Accepted Manuscripts are published online shortly after acceptance, before technical editing, formatting and proof reading. Using this free service, authors can make their results available to the community, in citable form, before we publish the edited article. We will replace this *Accepted Manuscript* with the edited and formatted *Advance Article* as soon as it is available.

You can find more information about *Accepted Manuscripts* in the [Information for Authors](#).

Please note that technical editing may introduce minor changes to the text and/or graphics, which may alter content. The journal's standard [Terms & Conditions](#) and the [Ethical guidelines](#) still apply. In no event shall the Royal Society of Chemistry be held responsible for any errors or omissions in this *Accepted Manuscript* or any consequences arising from the use of any information it contains.

^{14}N overtone transition in double rotation solid-state NMR

Ibraheem M. Haies^{a,b}, James A. Jarvis^c, Lynda J. Brown^a, Ilya Kuprov^a, Philip T.F. Williamson^c,
Marina Carravetta^{a,*}

^a School of Chemistry, University of Southampton, SO17 1BJ, Southampton, United Kingdom.

^b Department of Chemistry, College of Science, University of Mosul, Mosul, Iraq.

^c Centre for Biological Sciences, University of Southampton, SO17 1BJ, Southampton, United Kingdom.

ABSTRACT: Solid-state NMR transitions involving outer energy levels of the spin-1 ^{14}N nucleus are immune, to first order in perturbation theory, to the broadening caused by the nuclear quadrupole interaction. The corresponding overtone spectra, when acquired in conjunction with magic-angle sample spinning, results in lines which are just few kHz wide, permitting the direct detection of nitrogen compounds without the need for labeling. Despite the success of this technique, the “overtone” resonances are still broadened due to indirect, second order, effects arising from the large quadrupolar interaction. Here we demonstrate that another order of magnitude in spectral resolution may be gained by using double rotation. This brings the width of ^{14}N solid-state NMR lines much closer to the region commonly associated with high-resolution solid-state NMR spectroscopy of ^{15}N and demonstrates the improvements in resolution that may be possible through the development of pulsed methodologies to suppress these second order effect.

Introduction

Nitrogen is one of the most abundant elements in nature, but most nitrogen NMR studies have so far been restricted to the ^{15}N isotope (natural abundance $\sim 0.4\%$) to avoid problems associated with the large ^{14}N quadrupolar interaction, often in the MHz range¹⁻⁴. Significant attention has been given to the possibility of developing high-resolution versions of ^{14}N solid state NMR, to ease the acquisition of data without isotopic labelling, as well as to harvest additional information of the nitrogen site and its environment as provided by the quadrupolar interaction. This has led to the development of a number of promising techniques including ultra-wideband acquisition^{2, 3, 5}, indirect detection^{4, 6-14} and excitation of ^{14}N overtone transitions¹⁵⁻²⁴. Overtone NMR spectroscopy is advantageous because the width of the ^{14}N overtone powder pattern is unaffected, to first order in perturbation theory, by the quadrupolar interaction²⁵. The experimental feasibility of directly detecting the ^{14}N overtone transition by NMR was first demonstrated in the 1980's by Tycko and Opella on static samples^{21-23, 25}. More recently, ^{14}N overtone spectra acquired under magic-angle spinning (MAS) have been reported, demonstrating the existence of only five ^{14}N spinning sidebands^{17, 24}. However, even under MAS, the overtone powder line is still in the kHz range, due to the presence of quadrupolar interaction terms of spherical rank higher than 2 in the effective Hamiltonian. Any further improvements in resolution will necessitate the removal of these terms. Several methods exist for the elimination of high-rank quadrupole interaction terms. For half-integer quadrupolar nuclei, MQMAS²⁶⁻²⁸ and STMAS²⁹ methods remove them by modifying the spin part of the effective Hamiltonian. For

the spatial part, double rotation (DOR)³⁰⁻³² and dynamic angle spinning (DAS)^{31, 33} achieve the same objective by mechanical averaging.

One of the main challenges for the routine application of ¹⁴N solid state NMR is resolution. In this communication we address this issue and demonstrate experimentally that, when applied to ¹⁴N overtone NMR, DOR can bring about significant further reduction in line width and take the NMR lines into the sub-kHz domain more commonly associated with NMR of spin-1/2 nuclei. Information of the size of the quadrupolar interaction is still present in the DOR spectra as the peak position is determined by a combination of chemical shift and second order isotropic quadrupolar shift. A further challenge to tackle for methods for sensitivity enhancement are already being developed, including polarization transfer²⁴, DNP²⁰, optimal control theory³⁴ and other instrumental improvements.

We also report progress with another long-standing issue associated with both DOR and overtone spectroscopy – the mathematical complexity of its numerical treatment. This paper uses the Fokker-Planck formalism^{35, 36} (recently implemented in *Spinach*³⁷). Its most attractive feature is that the DOR evolution operator is time-independent and the rotor coordinates, once discretized, are in a direct product relationship with the spin degrees of freedom.

Materials and Methods

Solid State NMR. All the NMR measurements were performed on a Bruker AVANCE III 850 MHz spectrometer. All spectra were referenced indirectly to 0 ppm (liquid ammonia) using

the ^{14}N signal of ammonium chloride at 39.3 ppm³⁸. The overtone reference frequency was taken to be twice the ^{14}N reference frequency.

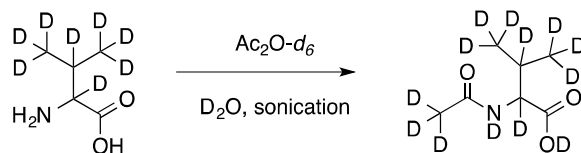
The DOR measurements used a wide-bore double resonance DOR probe, with diameters of 9.3 mm for the outer rotor (at magic angle) and 3.4 mm for the inner rotor (at 30.56°) respectively. Both rotors rotate in a clockwise direction. The power level was calibrated to give an overtone nutation frequency of $\omega_{nut}^{OT} / 2\pi = 21$ kHz for the ^{14}N overtone using the ^{17}O signal from H_2O sample at 115.262 MHz and no ^1H decoupling was used under DOR.

MAS measurements were performed using a 3.2 mm wide-bore triple resonance probe and 3.2 mm zirconium oxide rotor, which rotates in the anticlockwise direction. For MAS, SPINAL64 decoupling at $\omega_{nut}^H / 2\pi = 89$ kHz was used throughout, while the overtone nutation frequency was set to $\omega_{nut}^{OT} / 2\pi = 70$ kHz and calibrated on water as above.

NMR samples. DOR experiments were performed on 27 mg of glycine- N,N,O - d_3 (Aldrich) and 24 mg of N -(acetyl- d_3)valine- d_{10} (NAV, prepared in house). The synthesis and characterization of fully deuterated NAV, is described below. Deuterated samples were chosen for the DOR experiments due to the very limited ^1H decoupling performance of this probe. For the MAS measurements, 35 mg of natural abundance glycine and 31 mg of natural abundance NAV (both obtained from Sigma-Aldrich and used without further purifications) were used. During MAS acquisition, SPINAL-64 decoupling was used with nutation frequency of 89 kHz. All recycle delays were set to 0.5 s.

Synthesis of N -(acetyl- d_3)valine- d_{10} . Solvents and reagents were used as received from standard chemical suppliers unless otherwise stated. Fourier-transform infrared (FT-IR) spectra are reported in wavenumbers (cm^{-1}) and were collected on a Nicolet 380

spectrometer fitted with a Diamond platform. ^2H and ^{13}C NMR spectra were recorded in $\text{CH}_3\text{OH}/\text{CD}_3\text{OD}$ solutions (76.8 MHz and 100 MHz respectively). Chemical shifts are reported in δ units using and coupling constants (J) are reported in Hz and are rounded to the nearest 0.1 Hz. Melting points are uncorrected. Electrospray mass spectra were obtained using a Micromass platform mass analyser with an electrospray ion source.



Scheme 1³⁹

A clear solution was prepared by sonication of L-valine- d_8 (250 mg, 2 mmol) in D_2O (5 mL). Acetic anhydride- d_6 (433 mg, 4 mmol, 380 μL) was added at 0 min, 2 min and 4 min (127 μL at each interval). The reaction was sonicated for a further 5 min and then the solvent removed *in vacuo*. The white residue was dissolved in methanol (20 mL) and the solution filtered to remove traces of unreacted starting material. The filtrate was evaporated *in vacuo* and the residue recrystallised twice from D_2O (2 x 1 mL), to give *N*-(acetyl- d_3)valine- d_{10} as a white solid (280 mg, 1.63 mmol, 82%). Further details for the characterization of this material are provided in the Supporting Information.

Theory

The recently proposed Fokker-Planck formalism for solid state NMR calculations^{36, 38} allows the simulation of double rotation overtone NMR experiments to be performed without undue formulaic

complexity and in reasonable time. The primary observation is very similar to the one made in the stochastic Liouville equation theory^{40, 41} – spatial dynamics may be introduced into the equation of motion simply by adding the corresponding derivatives to the evolution generator. In the case of DOR NMR, we have:

$$\frac{\partial}{\partial t} \hat{\rho}(\varphi_0, \varphi_1, t) = \left[-i\hat{H}(\varphi_0, \varphi_1, t) + \omega_0 \frac{\partial}{\partial \varphi_0} + \omega_1 \frac{\partial}{\partial \varphi_1} \right] \hat{\rho}(\varphi_0, \varphi_1, t) \quad (1)$$

where $\varphi_{0,I}$ are outer and inner rotor angles, $\omega_{0,I}$ are outer and inner rotor angular frequencies, $\hat{\rho}(\varphi_0, \varphi_1, t)$ is the state vector and $\hat{H}(\varphi_0, \varphi_1, t)$ is the spin Hamiltonian commutation superoperator:

$$\hat{H}(\varphi_0, \varphi_1, t) = \hat{H}_0(\varphi_0, \varphi_1) + \hat{H}_1(t) \quad (2)$$

in which the dependence on the two spinner angles is parametric and the time-dependent part (radiofrequency pulses, *etc.*) is orientation-independent.

If the spatial basis is chosen to be complex exponentials of the rotor angles, this formalism would reduce³⁵ to nested Floquet theory^{42, 43}. Equation (1) does, however, also permit a more direct numerical approach – exact matrix representations exist for the derivative operators on any periodic grid⁴⁴. At the matrix level, this leads to remarkably simple relations:

$$\begin{aligned} \frac{\partial}{\partial t} \mathbf{\rho}(t) &= \mathbf{F}(t) \mathbf{\rho}(t), & \mathbf{F}(t) &= \mathbf{H}_0 + \mathbf{H}_1(t) + \mathbf{D}_1 + \mathbf{D}_0 \\ \mathbf{H}_1(t) &= \hat{E}_{N_0} \otimes \hat{E}_{N_1} \otimes \hat{H}_1(t), & \mathbf{D}_1 &= \hat{E}_{N_0} \otimes \hat{D}_{N_1} \otimes \hat{E}_{N_s}, & \mathbf{D}_0 &= \hat{D}_{N_0} \otimes \hat{E}_{N_1} \otimes \hat{E}_{N_s} \end{aligned} \quad (3)$$

where N_0 is the number of grid points for the outer rotor, N_1 is the number of grid points for the inner rotor, N_s is the dimension of the spin state space, \hat{E} are identity superoperators of indicated dimensions, \hat{D} are Fourier spectral differentiation matrices⁴⁴ of indicated dimensions, the vector $\mathbf{\rho}(t)$ is obtained by stacking state vectors $\hat{\rho}(\varphi_0^{(n)}, \varphi_1^{(k)}, t)$ vertically in the order of increasing index

of the inner rotor grid points, followed by the increasing index of the outer rotor grid points, and the block-diagonal matrix \mathbf{H}_0 is obtained by concatenating individual grid point Hamiltonians $\hat{H}_0(\varphi_0^{(n)}, \varphi_1^{(k)})$ in the same order as the state vectors.

From the practical programming perspective, the entire procedure is implemented and extensively annotated in the double rotation module of *Spinach*³⁷. At the cost of increasing the matrix dimension, the presence of the double rotation no longer troubles the end user – DOR dynamics operators are now just another static term in the background Hamiltonian \mathbf{F}_0 :

$$\mathbf{F}(t) = \mathbf{F}_0 + \mathbf{F}_1(t), \quad \mathbf{F}_0 = \mathbf{H}_0 + \mathbf{D}_1 + \mathbf{D}_O, \quad \mathbf{F}_1(t) = \mathbf{H}_1(t) \quad (4)$$

Another advantage of Equation (3) is that averages with respect to the phases of both rotors may be computed simply by taking the average of every block in $\rho(t)$. This means that a powder simulation would only need a two-angle spherical averaging grid. In principle, even that is not strictly necessary³⁷, but the mathematics in the grid-free case is less straightforward.

From this point onwards, the problem is identical to the simulation of a pulse-acquire experiment with a soft pulse, with the additional complication that the frequency of the pulse is *twice* the Larmor frequency of the spin – we are pulsing and detecting the overtone transition. The methods used to perform such simulations in reasonable time are described in our previous paper²⁴ and implemented in *Spinach*³⁷. Because the number of spinning sidebands in overtone spectra is small and the resulting signals are narrow, five to seven grid points for the discretization of the phase of each rotor and a rank 5 Lebedev spherical averaging grid (parallel evaluation) were in practice found to be sufficient. When the calculation is parallelized with respect to the spherical averaging grid, the simulation shown in Figure 1 takes a few minutes on a contemporary quad-core desktop workstation. All simulations for DOR and MAS experiments were performed using a single ¹⁴N spin and neglecting the effects of protons and deuterons, using parameters summarised in Table 1.

Hence the simulated DOR lineshapes are unaffected by the residual dipolar interactions to other neighbouring nuclei.

Results and discussion

DOR NMR spectra were simulated for N-acetylvaline (NAV) and glycine (Fig. 1) using spin Hamiltonian parameters given in Table 1. Under MAS, the spectrum consists of five sidebands, the strongest peak belonging to the +2 sideband for the counter-clockwise (it matters) spinner rotation direction¹⁷. Under DOR, each sideband is split into further family of sidebands whose linewidth is reduced compared to those obtained under MAS.

Experimental spectra (Fig. 1, inserts) of deuterated glycine- d_3 and NAV- d_{13} were acquired at 850 MHz on a Bruker Avance III spectrometer equipped with a DOR probe where both spinners rotate in a clockwise direction. Due to the limited excitation bandwidth, it is not possible to record the overall spectrum at once and only individual sidebands can be recorded. The overtone transition is forbidden in the Zeeman basis and overtone excitation is quite ineffective with the low power levels provided by the DOR probe, leading to long pulse length and narrow bandwidth. Nutation curves for the $(-2,-2)$ spinning sidebands of both compounds are given in Fig. S1. Glycine requires longer pulses than NAV due to smaller quadrupole coupling constant. As seen in Fig. 1, experimental results and simulation show good agreement for both the resonance position and relative peak intensity. The most intense signal is at the $(-2,-2)$ spinning sideband. Attempts were also made to acquire other DOR spinning sidebands for glycine (8000 scans) but there was no clear evidence of a signal (Fig. S2). The extent of the line-narrowing effect of DOR on overtone NMR data may be appreciated from Figs. 2 and 3. Notice that simulations are consistently much narrower than the experimental data. The larger experimental linewidth is attributed to spinning frequency

instabilities and dipolar couplings to other nuclei. Spinning speed variations of the DOR rotors were of the order of ± 25 Hz, and since we are observing not the center-band but sidebands of the overtone signal, unstable spinning will significantly broaden the resonances. Moreover, the DOR experiments were run at moderate spinning frequencies and without any decoupling, hence dipolar coupling to deuterium and protons are unlikely to be fully averaged out. Such an extended spin system is too complex for accurate numerical simulation. Simulations of DOR in Figs 2 and 3 are sharp as they do not suffer from these effects, as they assumed a single nitrogen atom, but the full quadrupolar Hamiltonian (not just first and second order terms) is considered here. The *Spinach* input file which generated Fig. 1 for glycine is included in the Supporting Information as an example. For glycine, both the experimental and the simulated DOR NMR lines at $(-2,-1)$ and $(-2,-2)$ sidebands are about three times narrower than the corresponding MAS lines (Fig. 2). The experimental width of the $(-2,-2)$ sideband under DOR is 280 Hz, while the width of the +2 spinning sideband under MAS is about 900 Hz (Fig. 2). It is clear from Fig. 3 that the $(-2,-2)$ DOR sideband is much sharper than the +2 MAS sideband for NAV also: 3.57 kHz line width under MAS is reduced to only 0.42 kHz under DOR, an improvement by almost an order of magnitude.

The reduction in line width observed under DOR indicates that the residual width apparent in the MAS ^{14}N overtone spectra does indeed arise from the second order quadrupolar terms in the Hamiltonian, removed in the DOR experiment. Importantly, none of that narrowing can be attributed to the narrow bandwidth of the very long overtone pulses under DOR, nor to the deuteration in the sample. This is because identical reduction in the linewidth is seen in the simulations in which the dipolar interactions with the surrounding

atoms is switched off and ideal, very strong pulses, are used (Fig. 1). The large number of scans required to record the DOR data arise from reduced sample volume and reduced excitation efficiency compared to the MAS experiments, where stronger RF pulses are possible¹⁶.

Conclusions

These DOR results demonstrate the potential of ¹⁴N double rotation overtone NMR in terms of resolution, with experimental line widths of a few hundred Hz achievable under DOR conditions. This represents a reduction by a factor of 3 and 9, as compared to MAS, for glycine and NAV respectively and reduction in linewidth (determined by the third-order quadrupolar terms that survive double rotation averaging) to just tens of Hz predicted from theoretical simulations when artificial broadening is switched off, which sets the theoretical limit of what can be achieved under ideal conditions, without the intrinsic hardware limitation of DOR probes. The ongoing experimental developments go side by side with recent advances in theoretical and computational modelling. It is now possible to simulate elaborate overtone pulse sequences and soft pulses under MAS and double rotation in reasonable time³⁷.

The routine application of DOR presents a number of technical challenges both in terms of sensitivity and RF performance. However pulsed methods for suppression of 2nd order quadrupolar broadening effects in the indirect dimension (MQMAS, STMAS) have existed for half-integer spins for some time and can be implemented using standard solid-state NMR probes²⁶⁻²⁹. Our findings highlight that for integer spin nuclei, such as the ¹⁴N case explored

herein, similar averaging of the second order quadrupolar broadening is feasible and the developments of pulsed methods will enable the routine realization of the significant resolution enhancements we have observed.

ACKNOWLEDGEMENTS

MC thanks the University Research Fellowship scheme from the Royal Society for support. LJB thanks the Royal Society for a Dorothy Hodgkin fellowship. Ibraheem Haies thanks The Higher Committee for Education Development in Iraq for financial support. The UK 850 MHz solid-state NMR Facility instruments used in this research were funded by EPSRC and BBSRC, as well as the University of Warwick, including via part funding through Birmingham Science City Advanced Materials Projects 1 and 2 supported by Advantage West Midlands (AWM) and the European Regional Development Fund (ERDF). The authors acknowledge the use of the IRIDIS High Performance Computing Facility, and associated support services at the University of Southampton, in the completion of this work. The development of *Spinach* is supported by EPSRC (EP/H003789/1).

REFERENCES

1. L. A. O'Dell, *Prog. Nucl. Magn. Reson. Spectrosc.*, 2011, 59, 295-318.
2. T. Giavani, H. Bildsøe, J. Skibsted and H. J. Jakobsen, *J. Magn. Reson.*, 2004, 166, 262-272.
3. R. W. Schurko, *Acc. Chem. Res.*, 2013, 46, 1985-1995.
4. S. Cavadini, *Prog. Nucl. Magn. Reson. Spectrosc.*, 2010, 56, 46-77.
5. L. A. O'Dell and C. I. Ratcliffe, *Chem Commun (Camb)*, 2010, 46, 6774-6776.
6. S. Cavadini, A. Abraham and G. Bodenhausen, *Chem. Phys. Lett.*, 2007, 445, 1-5.
7. S. Cavadini, A. Abraham and G. Bodenhausen, *J Magn Reson*, 2008, 190, 160-164.
8. S. Cavadini, S. Antonijevic, A. Lupulescu and G. Bodenhausen, *J Magn Reson*, 2006, 182, 168-172.
9. S. Cavadini, S. Antonijevic, A. Lupulescu and G. Bodenhausen, *Chemphyschem*, 2007, 8, 1363-1374.
10. S. Cavadini, A. Lupulescu, S. Antonijevic and G. Bodenhausen, *J. Am. Chem. Soc.*, 2006, 128, 7706-7707.
11. S. Cavadini, V. Vitzthum, S. Ulzega, A. Abraham and G. Bodenhausen, *J Magn Reson*, 2010, 202, 57-63.
12. Z. Gan, *J. Am. Chem. Soc.*, 2006, 128, 6040-6041.
13. Z. Gan, J. P. Amoureux and J. Trébosc, *Chem. Phys. Lett.*, 2007, 435, 163-169.
14. J. A. Jarvis, I. M. Haies, P. T. Williamson and M. Carravetta, *Phys. Chem. Chem. Phys.*, 2013, 15, 7613-7620.
15. D.-K. Lee and A. Ramamoorthy, *Chem. Phys. Lett.*, 1998, 286, 398-402.
16. Y. Nishiyama, M. Malon, Z. Gan, Y. Endo and T. Nemoto, *J Magn Reson*, 2013, 230, 160-164.
17. L. A. O'Dell and A. Brinkmann, *J. Chem. Phys.*, 2013, 138, 064201.
18. L. A. O'Dell, R. L. He and J. Pandohee, *Crystengcomm*, 2013, 15, 8657-8667.
19. L. A. O'Dell and C. I. Ratcliffe, *Chem. Phys. Lett.*, 2011, 514, 168-173.
20. A. J. Rossini, L. Emsley and L. A. O'Dell, *Phys. Chem. Chem. Phys.*, 2014, 16, 12890-12899.
21. R. Tycko and S. J. Opella, *J. Am. Chem. Soc.*, 1986, 108, 3531-3532.
22. R. Tycko and S. J. Opella, *J. Chem. Phys.*, 1987, 86, 1761.
23. R. Tycko, P. L. Stewart and S. J. Opella, *J. Amer. Chem. Soc.*, 1986, 108, 5419-5425.
24. I. Haies, J. Jarvis, H. Bentley, I. Heinmaa, I. Kuprov, P. Williamson and M. Carravetta, *Phys. Chem. Chem. Phys.*, 2015, DOI: 10.1039/c4cp03994g.
25. M. Bloom and M. A. LeGros, *Can. J. Phys.*, 1986, 64, 1522-1528.
26. L. Frydman and J. S. Harwood, *J. Am. Chem. Soc.*, 1995, 117, 5367-5368.
27. A. Medek, J. S. Harwood and L. Frydman, *J. Am. Chem. Soc.*, 1995, 117, 12779-12787.
28. G. Wu, D. Rovnyank, B. Q. Sun and R. G. Griffin, *Chem. Phys. Lett.*, 1996, 249, 210-217.
29. Z. H. Gan, *J. Am. Chem. Soc.*, 2000, 122, 3242-3243.
30. A. Samoson, E. Lippmaa and A. Pines, *Mol. Phys.*, 1988, 65, 1013-1018.
31. B. F. Chmelka, K. T. Mueller, A. Pines, J. Stebbins, Y. Wu and J. W. Zwanziger, *Nature*, 1989, 339, 42-43.
32. A. Samoson and A. Pines, *Rev. Sci. Instrum.*, 1989, 60, 3239-3241.
33. K. T. Mueller, B. Q. Sun, G. C. Chingas, J. W. Zwanziger, T. Terao and A. Pines, *J. Magn. Reson.*, 1990, 86, 470-487.
34. P. de Fouquieres, S. G. Schirmer, S. J. Glaser and I. Kuprov, *J. Magn. Reson.*, 2011, 212, 412-417.
35. L. J. Edwards, D. V. Savostyanov, A. A. Nevzorov, M. Concistre, G. Pileio and I. Kuprov, *J. Magn. Reson.*, 2013, 235, 121-129.
36. A. A. Nevzorov, *J. Magn. Reson.*, 2014, 249.
37. H. J. Hogben, M. Krzystyniak, G. T. Charnock, P. J. Hore and I. Kuprov, *J. Magn. Reson.*, 2011, 208, 179-194.

38. P. Bertani, J. Raya and B. Bechinger, *Solid State Nucl. Magn. Reson.*, 2014, 61-62, 15-18.
39. M. Erdelyi, V. Langer, A. Karlen and A. Gogoll, *New J. Chem.*, 2002, 26, 834-843.
40. G. Moro and J. H. Freed, *J Chem Phys*, 1981, 74, 3757-3773.
41. C. F. Polnaszek, G. V. Bruno and J. H. Freed, *J Chem Phys*, 1973, 58, 3185-3199.
42. M. Leskes, P. K. Madhu and S. Vega, *Prog Nucl Mag Res Sp*, 2010, 57, 345-380.
43. I. Scholz, J. D. van Beek and M. Ernst, *Solid State Nucl Mag*, 2010, 37, 39-59.
44. L. N. Trefethen, *Spectral methods in MATLAB*, Siam, 2000.
45. R. A. Haberkorn, R. E. Stark, H. Vanwilligen and R. G. Griffin, *J Am Chem Soc*, 1981, 103, 2534-2539.
46. R. E. Taylor and C. Dybowski, *J. Mol. Struct.*, 2008, 889, 376-382.
47. R. E. Stark, R. A. Haberkorn and R. G. Griffin, *J. Chem. Phys.*, 1978, 68, 1996.
48. E. Salnikov, P. Bertani, J. Raap and B. Bechinger, *J Biomol Nmr*, 2009, 45, 373-387.
49. M. Bak, R. Schultz, T. Vosegaard and N. C. Nielsen, *J Magn Reson*, 2002, 154, 28-45.
50. G. Hou, I. J. Byeon, J. Ahn, A. M. Gronenborn and T. Polenova, *J. Chem. Phys.*, 2012, 137, 134201.

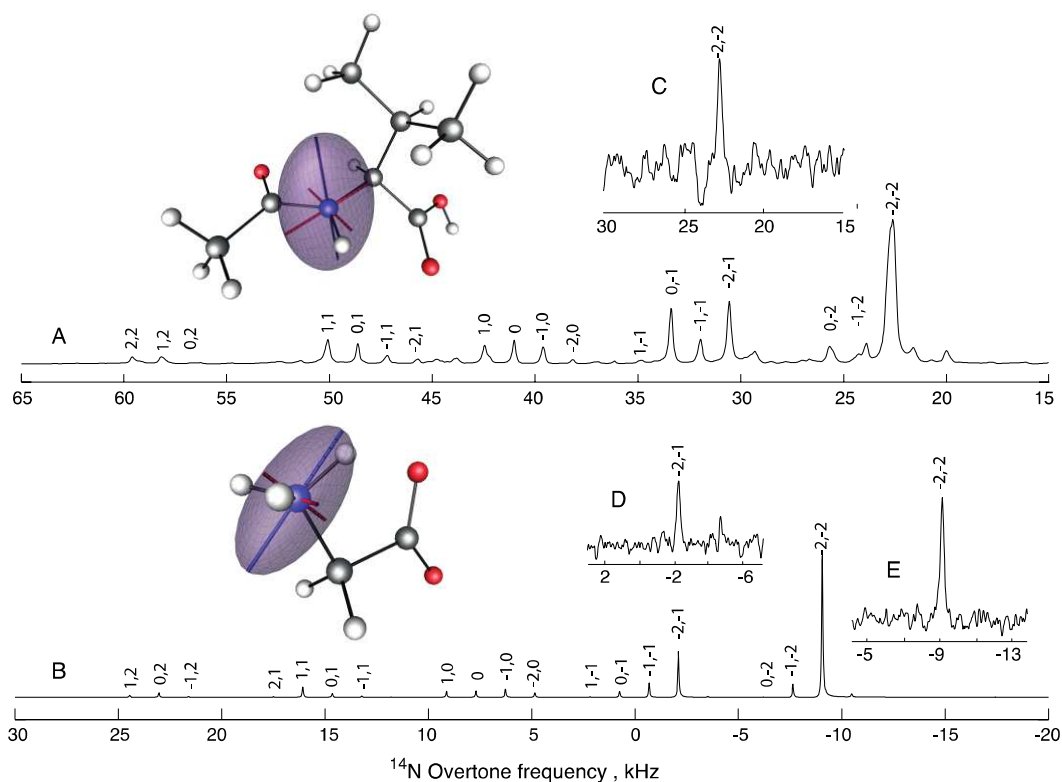


FIGURE 1: DOR simulation and experiments for the ^{14}N overtone transition of glycine and NAV. Simulations were obtained using one ^{14}N spin, parameters from Table 1 and ideal pulses. Experiments were recorded with $\omega_{\text{nut}}^{\text{OT}} / 2\pi = 21$ kHz without decoupling. The numbers above the peaks are indices for spinning sidebands of the outer and inner rotors respectively. (A) Simulation for NAV using outer rotor frequency of 1.45 kHz and inner rotor frequency of 7.6 kHz; (B) Simulation for glycine using outer rotor frequency of 1.425 kHz and inner rotor frequency of 6.95 kHz; (C) Experimental spectrum of the $(-2,-2)$ spinning sideband of deuterated NAV acquired with 550,000 scans using 300 μs pulse width; (D-E) Experimental spectra of the $(-2,-2)$ and $(-2,-1)$ spinning sidebands of deuterated glycine respectively,

acquired with 40,000 scans using 800 μ s pulse width. The ellipsoid plots indicate the principal directions and the absolute values of the corresponding eigenvalues for the ^{14}N NQR tensors.

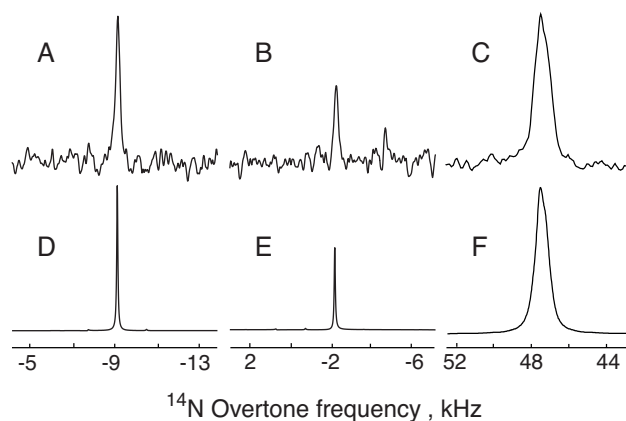


FIGURE 2: Line width comparison for DOR and MAS overtone powder spectra of glycine. (A) DOR experiment for the $(-2,-2)$ sideband of deuterated glycine, 40000 scans, no decoupling; (B) DOR experiment for the $(-2,-1)$ sideband of deuterated glycine, 40000 scans, no decoupling; DOR conditions are specified in Fig. 1 caption. (C) MAS experiment for the +2 spinning sideband of glycine, 1024 scans, SPINAL64 decoupling, using $\omega_{\text{nut}}^{\text{OT}} / 2\pi = 70$ kHz and a 275 μs excitation pulse with $\omega_e / 2\pi = 19.84$ kHz. (D-F) Simulations of the data in A-C were performed using one ^{14}N spin, the parameters given in Table 1, using durations and amplitudes matching the experimental data.

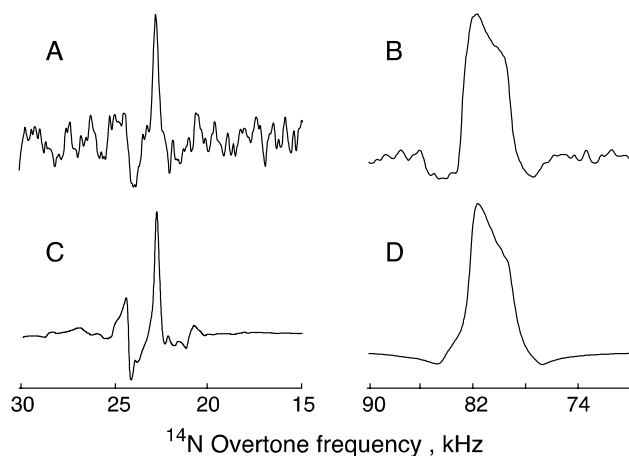


FIGURE 3: Line width comparison for DOR and MAS overtone powder spectra of NAV. (A) DOR experiment data for the $(-2,-2)$ spinning sideband of deuterated NAV, 550000 scans, no decoupling. DOR conditions are specified in Fig. 1 caption. (B) MAS experiment at the +2 spinning sideband of NAV, 40000 scans, SPINAL64 decoupling, using $\omega_{nut}^{OT} / 2\pi = 70$ kHz and a $275 \mu\text{s}$ excitation pulse with $\omega_r / 2\pi = 19.84$ kHz; (C) and (D) are the corresponding simulations, using one ^{14}N spin, the parameters in given in Table 1, using durations and amplitudes matching the experimental data. Notice that the two features on the side on the main peak in (A) and (C) are spinning sidebands of the outer rotor.

Table 1. Summary of parameters used for the simulations for glycine and NAV, using a single nitrogen spin. CSA interaction tensor orientations are quoted relative to the eigenframe of the ^{14}N quadrupolar interaction tensor. Inner and outer rotor speed match the experimental data. Floquet theory convergence is achieved at rank 5 in the MAS simulations, also rank 5 was used for the inner and the outer rotation in the DOR simulations.

	C_q MHz	η_q	σ_{iso} ppm	$\Delta\sigma$ ppm	η	Euler angles, CSA	Lebedev Grid Rank	(ν_{out}, ν_{in}) kHz
Gly ^{45, 46}	1.18	0.53	32.4	–	–	–	11	(1.425, 6.95)
NAV ⁴⁷⁻⁵⁰	3.21	0.32	121.8	105	0.23	[–90,–90,–17]	65	(1.450, 7.60)